Penetration kinetics of dimethyl sulphoxide and glycerol in dynamic optical clearing of porcine skin tissue *in vitro* studied by Fourier transform infrared spectroscopic imaging

Jingying Jiang
Tianjin University
State Key Laboratory of Precision Measuring Technology and Instruments
Tianjin 300072, China
and
Tianjin University
Department of Biomedical Engineering
College of Precision Instruments and Opto-Electronics
Tianjin 300072, China

Matthias Boese
Bruker Optik GmbH
Biomedical Products
D-76275 Ettlingen, Germany

Paul Turner
Bruker Optics Limited
Coventry CV4 9GH, England

Ruikang K. Wang
Oregon Health and Science University
Department of Biomedical Engineering
Beaverton, Oregon 97006

Abstract. By use of a Fourier transform infrared (FTIR) spectroscopic imaging technique, we examine the dynamic optical clearing processes occurring in hyperosmotically biocompatible agents penetrating into skin tissue *in vitro*. The sequential collection of images in a time series provides an opportunity to assess penetration kinetics of dimethyl sulphoxide (DMSO) and glycerol beneath the surface of skin tissue over time. From 2-D IR spectroscopic images and 3-D false color diagrams, we show that glycerol takes at least 30 min to finally penetrate the layer of epidermis, while DMSO can be detected in epidermis after only 4 min of being topically applied over stratum corneum sides of porcine skin. The results demonstrate the potential of a FTIR spectroscopic imaging technique as an analytical tool for the study of dynamic optical clearing effects when the bio-tissue is impregnated by hyperosmotically biocompatible agents such as glycerol and DMSO.
[DOI: 10.1117/1.2899153]

Keywords: penetration kinetics; dynamic optical clearing; Fourier transform infrared spectroscopic imaging; biocompatible chemical agents.

Paper 07225SSR received Jun. 20, 2007; revised manuscript received Nov. 6, 2007; accepted for publication Nov. 22, 2007; published online Mar. 26, 2008.

1 Introduction

The effects of optical clearing of highly scattering biological tissue by use of hyperosmotically biocompatible agents have been observed by using a number of techniques,[1–10] examples of which include near-infrared spectrophotometers,[2,3] optical coherence tomography (OCT) imaging,[4–6] charge-coupled device (CCD) cameras[7] for direct observation, mass loss assessment,[7] transdermal skin resistance (TSR) measurement,[8] and second harmonic generation imaging.[10] The existing results are encouraging, since they demonstrate that the addition of hyperosmotically biocompatible agents such as glycerol,[5,8,10] propylene glycol,[2,5,6] DMSO,[2,8] glucose,[4] oleic acid,[7] or dextrose[9] may lead to turbid tissue (for example skin, gastrointestinal tissue, and sclera or aorta), becoming optically clear. The explanations for optical improvements brought by optical clearing were proposed as the creation of a better refractive index matching environment induced by dehydration and structural reorganization within the tissue, which could lead to the reduction of light scattering.

Despite numerous studies being performed to demonstrate the optical clearing effect within highly scattering biological tissue after application of the biocompatible chemical agents, our understanding of the actual clearing mechanisms involved is still relatively poor. To facilitate the availability of the optical clearing technique in the enhancement of light penetration depth and in the improvement of imaging performance for high-resolution imaging of biological tissue, there is a need to perform further systematic studies to delineate accurate mechanisms of the dynamic optical clearing process. In this regard, penetration kinetics in the tissue clearing process, i.e., the penetration characteristics of hyperosmotically biocompatible agents within tissue, should be examined in the first place. For this aim, new analytical tools need to be introduced.

Spectroscopic imaging is an attractive method, since it can provide simultaneous information on both spatial and chemical properties of an intact system while preserving the sample integrity. By taking advantage of the vibrational spectral signatures of biological components, such as lipids and proteins, it is possible to obtain images of the intrinsic distribution of these molecules. Fourier transform infrared (FTIR) spectroscopic imaging with focal plane array (FPA) detectors for spectroscopic detection is a relatively new technique that is capable of real-time microscopic chemical characterizations.[11] As opposed to conventional FTIR microspectroscopic instrumentation that employs a single detection element hundreds of micrometers in size,[11] spectral multiplexing combined with multichannel detection in a FTIR interferometer, microscope, and FPA assembly enables spectroscopic and spatial discrimi-

1083-3668/2008/13(2)/021105/7/$25.00 © 2008 SPIE

nation over a sample field of view in minutes.[11] To date, FTIR spectroscopic imaging has been used to examine a variety of polymers and biological systems.[12,13] The good chemical specificity of FTIR spectroscopic imaging would allow the analysis of a broader range of pharmaceuticals. Furthermore, FTIR spectroscopic imaging has a relatively high spatial resolution down to 4 μm and the possibility of accurate quantification. The fast acquisition required for an FTIR spectroscopic imaging experiment allows a time resolution on the order of minutes. This time resolution has enabled the study of polymer dissolution by solvents[14,15] and the study of transdermal drug delivery systems.[16] Therefore, FTIR spectroscopic imaging could be a good candidate for the study of penetration kinetics of dynamic optical clearing processes.

The objectives of this study were to 1. determine the feasibility of FTIR spectroscopic imaging techniques as an analytical tool for the investigation of optical clearing by use of hyperosmotic agents, and 2. examine the penetration kinetics of dimethyl sulphoxide (DMSO) and glycerol within tissue during optical clearing processes. For these aims, we examined two hyperosmotically biocompatible agents, i.e., 50% DMSO/distilled water (v/v) and 80% glycerol/distilled water (v/v) solutions, for their dynamic optical clearing effect on porcine skin tissue after topical applications. The sequential collection of images in a time series has been obtained by a FTIR spectroscopic imaging technique, which provides good opportunity to assess the penetration kinetics of glycerol and DMSO beneath the surface of skin tissue over time.

2 Materials and Methods

2.1 *Tissue Sample Preparation*

Fresh porcine skin was obtained from an accredited slaughter house with removal of muscle and fat tissue layers using a scalpel blade. After depilation, porcine skin was cut in 20 $\times$ 20-mm pieces. The sample pieces were immediately sealed in a plastic bag to prevent them from natural dehydration, and kept frozen in a freezer at $-80\,^{\circ}$C until sectioning. Sections with the thickness of 1 mm were cut along the vertical direction of stratum corneum on a cryostat prior to performing FTIR spectroscopic imaging experiments. 30 minutes was allowed for samples left under room temperature before each measurement.

2.2 *Preparation of Hyperosmotically Biocompatible Agents*

DMSO and glycerol were chosen in this study, not only because they are common biocompatible agents that are used currently for optical clearing of tissue, but also because they possess different penetration characteristics within tissue, with DMSO having a much faster diffusion rate than glycerol.[17,18] Anhydrous DMSO and glycerol were purchased from Sigma Chemical Company, Saint Louis, Missouri. In this study, 50% DMSO and 80% glycerol solutions mixed with the distilled water (v/v) were prepared for FTIR spectroscopic imaging measurements.

2.3 *Data Acquisition and Analyses*

The imaging setup used in this study consisted of a step-scan spectrometer (Bruker IFS-66/s), a 64 $\times$ 64 HgCdTe (MCT) focal plane array (MCT-FPA) detector, and Hyperion 3000 microscope (Bruker Optics, Germany) with a NIR source and CaF_2 beamsplitter. All experiments were carried out in transmittance mode within the spectral range of 7500 to 3800 cm^{-1} at 16-cm^{-1} spectral resolution and 8-μm (2 $\times$ 2 pixel binning) spatial resolution. A 15$\times$ Cassegrain objective was used to image a sample area field of view (270 μm^2) onto a 64 $\times$ 64 pixel MCT-FPA that is equipped with an optimal-sized cold shield. The total data collection time per each individual image (nine scans) was approximately two minutes.

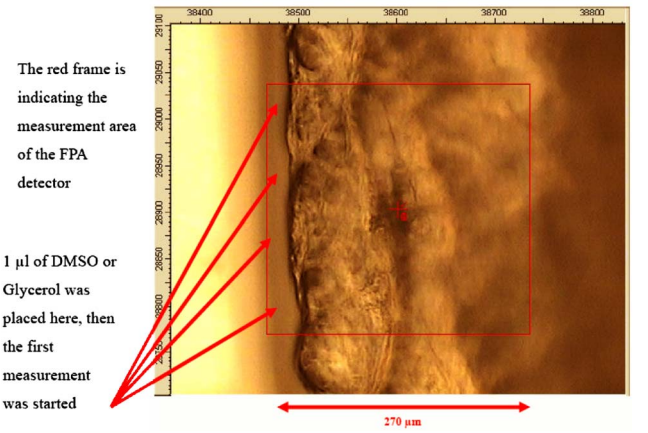

Fig. 1 Video image of the measured area of porcine skin. (Color online only.)

Figure 1 shows a video image of porcine skin, where the area marked by the box indicates the measured area of the MCT-FPA detector. A small volume (1 μl) of DMSO or glycerol solution was applied on the stratum corneum side of the porcine skin (indicated by arrows), and then the continuous measurements were immediately initiated. All data analysis was performed with OPUS/3D (Bruker Optics, Germany). Using OPUS/3D, the data can be visualized as diverse 2-D IR spectroscopic images and/or 3-D false color plots.

In addition, spectral measurements of intact porcine skin, pure DMSO, and anhydrous glycerol were performed with single element detectors on Hyperion 3000 to identify the marker bands for different species so that the spectroscopic imaging can be specific, i.e., the spectroscopic imaging can be more meaningful by integration of the signals within the marker bands. Figure 2 shows the spectral results measured within the range of 7500 to 3800 cm^{-1}. The red ellipses in the figures are indicating the marker bands, that is, 4750 to 4500 cm^{-1} for pig skin, 4500 to 4360 cm^{-1} for pure DMSO, and 4900 to 4600 cm^{-1} for anhydrous glycerol.

3 Results

3.1 *Penetration Kinetics of Dimethyl Sulphoxide within Porcine Skin*

3.1.1 *Marker bands for porcine skin and dimethyl sulphoxide*

The FTIR spectroscopic imaging technique gave a set of three dimensional data with *x-y* of the specimen size and the *z* dimension being the spectroscopic signal, i.e., wavenumber

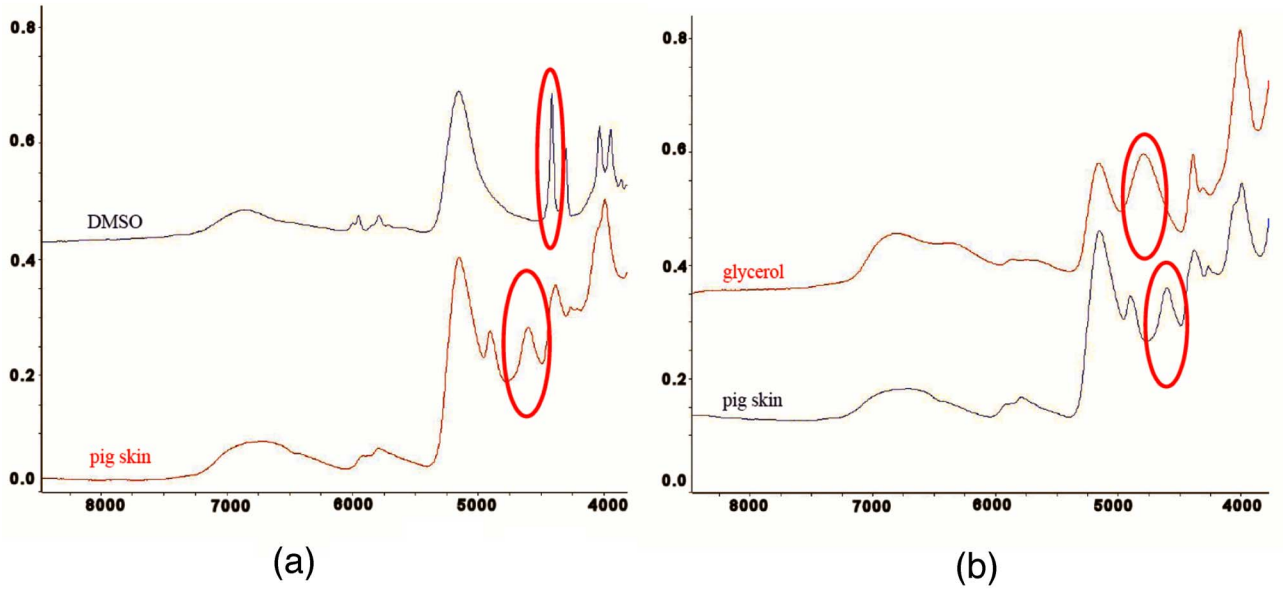

Fig. 2 Spectra of skin, DMSO, and glycerol between 7500 to 3800 cm^{-1} measured by FTIR microscope. (a) Spectra of DMSO and porcine skin, where the red ellipse indicates the marker band of 4750 to 4500 cm^{-1} for the skin and 4500 to 4360 cm^{-1} for DMSO. (b) Spectra of glycerol and porcine skin, where the red ellipse indicates the marker band of 4750 to 4500 cm^{-1} for the skin and 4900 to 4600 cm^{-1} for glycerol. (Color online only.)

axis. Figure 3 illustrates IR spectroscopic images and spectra of porcine skin impregnated with 50% DMSO solution, and also shows the marker bands of spectra: 4750 to 4500 cm^{-1} for the skin and 4500 to 4360 cm^{-1} for DMSO. Figures 3(a) and 3(b) are the collapsed images into the *x*-*y* plane by integration of the spectroscopic signal within the marker band for skin and DMSO. The plots in Figs. 3(c) and 3(d) show the spectroscopic signal at the points indicated in Figs. 3(a) and 3(b). Within 4750 to 4500 cm^{-1} for a porcine skin marker band, three possible bonds may be responsible for the spectral peak, i.e., the straight carbon chain and cis-double bands (4761 to 4545 cm^{-1}), the combination of CH_2 vibrations of protein side chains (4608 cm^{-1}), and vibration of C-H bonds bound to various fatty acids (4651 and 4566 cm^{-1}). For DMSO marker bands within 4500 to 4360 cm^{-1}, the spectral

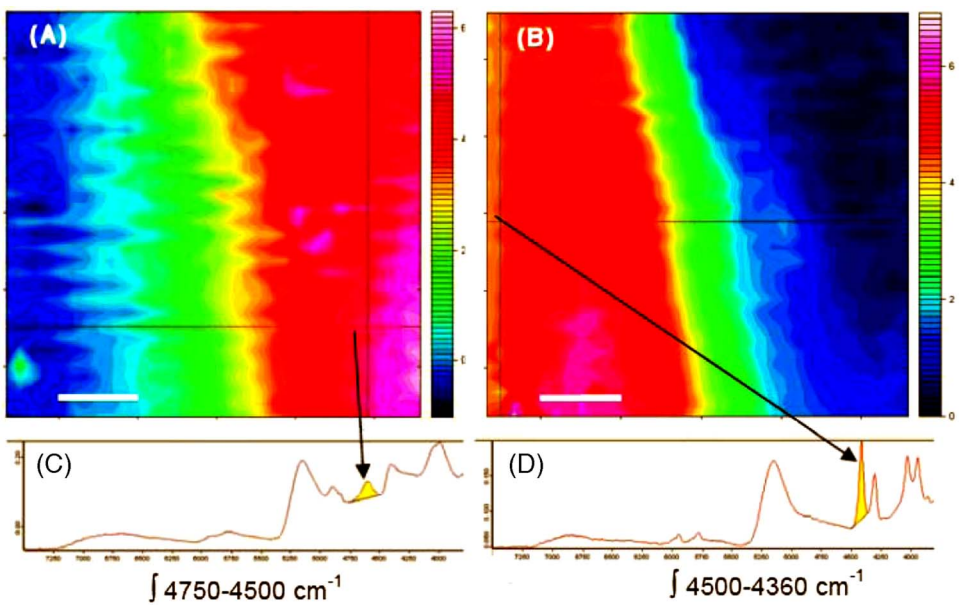

Fig. 3 IR spectroscopic images and marker bands for porcine skin and DMSO. (a) and (b) are the *x*-*y* collapsed images by integrating spectroscopic signal within the marker band for skin and DMSO, respectively. The plots (c) and (d) show the spectroscopic signals at the points indicated in (a) and (b). The scale bar indicates 50 μm. (Color online only.)

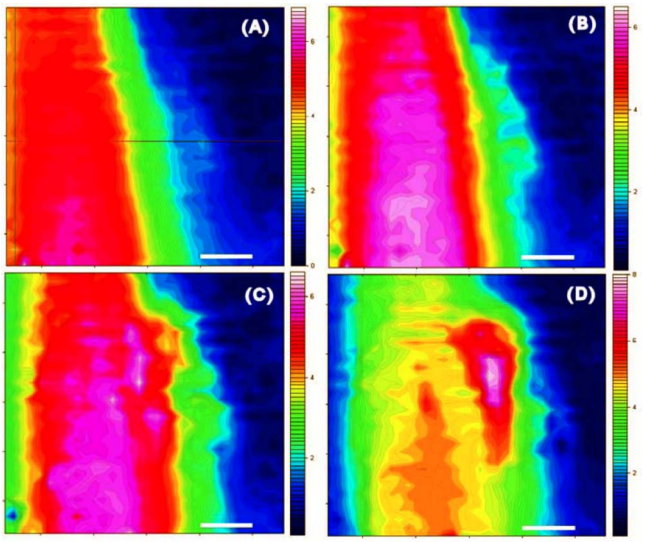

Fig. 4 Dynamic penetration processes of DMSO into porcine skin-monitored by FTIR imaging microscope at times (a) 0, (b) 4, (c) 12, and (d) 40 min, respectively. Scale bar indicates 50 μm. (Color online only.)

peak could derive from the N-H peptide and amino acids (4492 cm^{-1}).

3.1.2 *Infrared spectroscopic images for penetration kinetics of dimethyl sulphoxide*

Figure 4 demonstrated the dynamic penetration process of 50% DMSO/distilled water(v/v) solution into the porcine skin. A series of IR spectroscopic images over the time course within the range of 4500 to 4360 cm^{-1} were obtained by the FTIR spectroscopic imaging technique. Four representative images, start time [Fig. 4(a), at the time right after placing the DMSO on the skin], 4 min [Fig. 4(b)], 12 min [Fig. 4(c)], and 40 min [Fig. 4(d)], are shown in the figure. From Fig. 4, it can be seen that DMSO already penetrated into the epidermis layer after 4 min [Fig. 4(b)] of being placed on the stratum corneum side of porcine skin. With the elapse of time, DMSO continued penetrating into the superficial layer of dermis after 12 min [Fig. 4(c)], and finally into the deep layer of dermis after 40 min [Fig. 4(d)].

3.1.3 *Three dimensional false color plots for penetration kinetics of dimethyl sulphoxide*

3-D false color plots and contours at start time and after 40 min for 50% DMSO/distilled water(v/v) into porcine skin are shown in Fig. 5. From Fig. 5, it can be seen that DMSO dynamically penetrated into the deep layer (at more than 200 μm) of porcine skin.

3.2 *Penetration Kinetics of Glycerol within Porcine Skin*

3.2.1 *Marker bands for porcine skin and glycerol*

Similar to that described in Sec. 3.1.1, Fig. 6 illustrates IR spectroscopic images and spectra of porcine skin impregnated with 80% glycerol solution, and also shown are the marker bands of spectra: 4750 to 4500 cm^{-1} for the skin and 4900 to 4600 cm^{-1} for glycerol. Figures 6(a) and 6(b) are the collapsed images into the *x-y* plane by integration of the spectroscopic signal within the marker band for skin and glycerol, respectively. Figures 6(c) and 6(d) show the spectroscopic signal at the points indicated in Figs. 6(a) and 6(b). For glycerol, marker band within 4900 to 4600 cm^{-1}, the O-H deformation and C-O stretch of the third overtone (4761 cm^{-1}) could motivate the spectral peak within the range.

3.2.2 *Infrared spectroscopic images for penetration kinetics of glycerol*

Figure 7 illustrates the dynamic penetration process of 80% glycerol solution into porcine skin. A series of IR spectro-

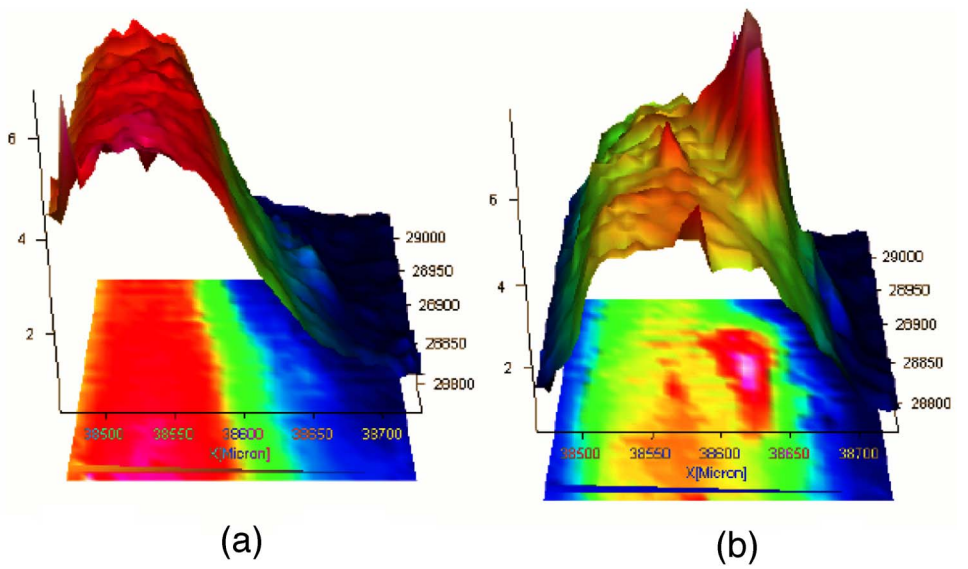

Fig. 5 3-D plots showing penetration kinetics of DMSO into porcine skin tissue, at times (a) 0 and (b) 40 min, respectively. (Color online only.)

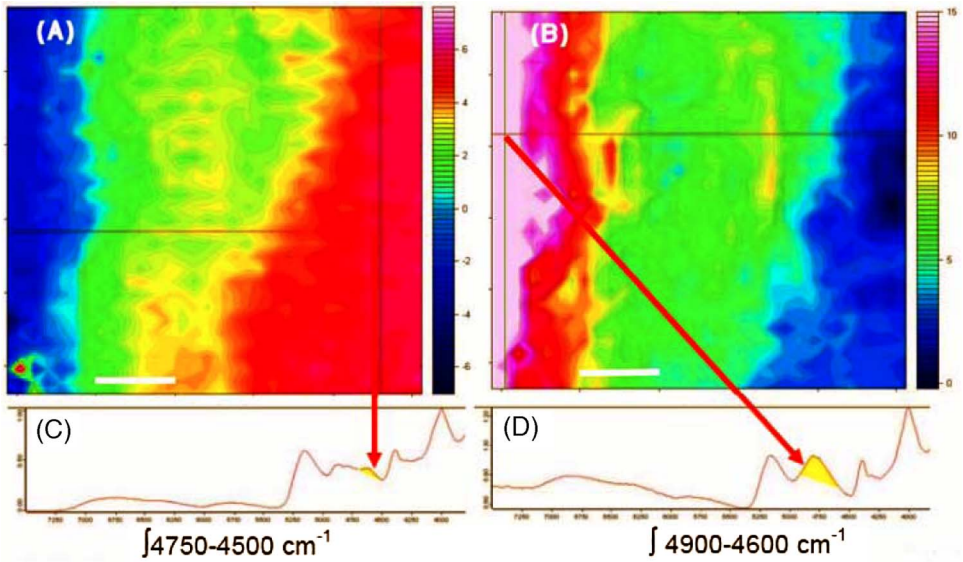

Fig. 6 IR spectroscopic images and marker bands for porcine skin and glycerol. (a) and (b) are the *x-y* collapsed images by integrating spectroscopic signal within the marker band for skin and glycerol, respectively. And plots (c) and (d) show the spectroscopic signals at the points indicated in (a) and (b). Scale bar indicates 50 μm. (Color online only.)

scopic images within 4900 to 4600 cm^{-1} in the course of time were obtained by a FTIR imaging microscope. Four representative images, start time [Fig. 7(a) right after application of the glycerol onto the skin surface], 4 min [Fig. 7(b)], 15 min [Fig. 7(c)], and 30 min [Fig. 7(d)], are shown in the figure. From Fig. 7, it can be seen that glycerol penetrated slowly into skin tissue. Only after 15 min, the slight changes in IR images appeared. 30 min later, it seemed that glycerol finally penetrated into the layer of epidermis (at around 70 μm). No further penetration action could be seen.

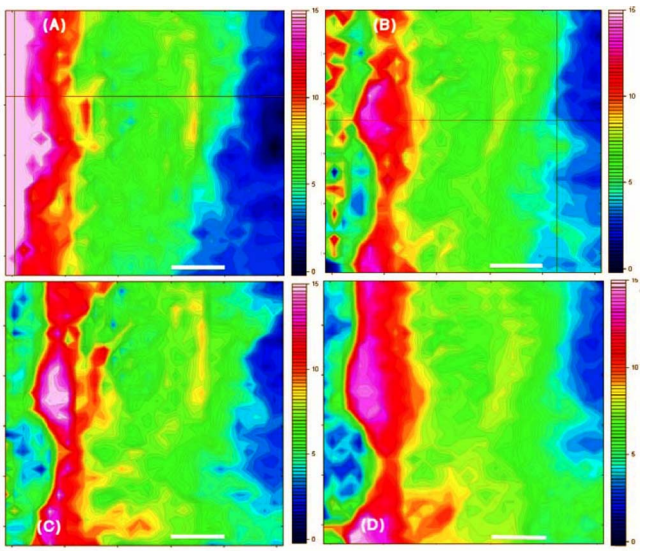

Fig. 7 Dynamic penetration processes of glycerol into porcine skin monitored by FTIR imaging microscope at times (a) 0, (b) 4, (c) 12, and (d) 40 min, respectively. Scale bar indicates 50 μm. (Color online only.)

3.2.3 *Three dimensional false color plots for penetration kinetics of dimethyl sulphoxide*

3-D false color plots and contours at start time and after 30 min for 80% glycerol/distilled water (v/v) into porcine skin are shown in Fig. 8. From Fig. 8, it can be seen that glycerol slowly penetrated into porcine skin, since it could be examined only in the superficial layer (at ~70 μm) even after 30-min penetration.

4 Discussion

In this study, by using the FTIR spectroscopic imaging technique, we have investigated for the first time the penetration kinetics of hyperosmotically biocompatible agents such as DMSO and glycerol during the optical clearing process of porcine skin. First of all, the presented results revealed that both DMSO and glycerol could to some degree penetrate into porcine skin. Moreover, both anhydrous glycerol and DMSO have the higher refractive index of 1.47, which is near to that of collagen. Thus, when they diffuse into tissue fluid, they can cause an increase in the refractive index of the fluid; therefore, the reduced scattering coefficient decreases, leading to an increase in light penetration, as shown in the previous experimental results.[19]

Furthermore, DMSO, a dipolar aprotic solvent, has a tendency to accept rather than donate protons. DMSO has been extensively studied previously as a carrier to enhance the percutaneous penetration of drugs through human skin[20] and guinea pig skin.[21] Since Stoughton and Fritsch[22] reported that DMSO can be used to enhance the percutaneous penetration of various agents in 1964, this characteristic has been exploited clinically in many different circumstances. By employing DMSO, Kolb et al.[17] evaluated the absorption and distribution of DMSO in small animals and humans. They

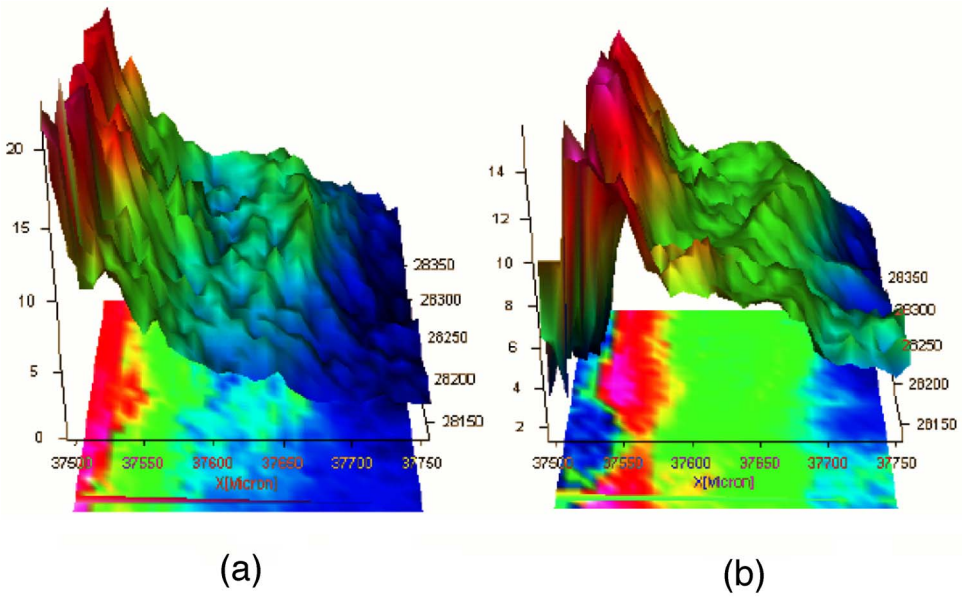

Fig. 8 3-D plots showing penetration kinetics of glycerol into porcine skin tissue at times (a) 0 and (b) 40 min, respectively. (Color online only.)

reported that 10 min after cutaneous application in the rat, radioactivity was measured in the blood. In humans, radioactivity appeared in the blood 5 min after cutaneous application. These findings indicate that the DMSO penetration happens within a very short time. The fast penetration rate of DMSO could decrease the osmolarity of the solution rapidly, even if the original one is high. He and Wang[19] demonstrated that DMSO has a fast penetration rate into tissue and therefore could bring enhancement in the penetration depth of light within tissue than other optical clearing agents. This is confirmed by the experimental results shown in Figs. 4 (IR spectroscopic images) and 5 (3-D false color plot, indicating the magnitude of the integrated signal fallen within the wavenumber range versus *x-y* coordinates of the sampling area).

Glycerol is biologically inert and is generally considered a safe additive by the Food and Drug Administration. It is widely used in the commercial formulations of foods, drugs, and cosmetics. He and Wang[19] reported that, compared to with DMSO, glycerol could be the best choice for improvement in optical imaging performance. However, it is difficult for glycerol alone to penetrate into the stratum corneum because of the hydrophilicity of glycerol, as the results shown in Figs. 7 (IR spectroscopic images) and 8 (3-D false color plots) by FTIR spectroscopic imaging technique demonstrated.

Figure 9 shows the penetration depth of DMSO and glycerol into porcine skin over the time course measured from the FTIR images. From Fig. 9, the penetration rate of DMSO within porcine skin was estimated as 37.5 μm/min within the first 4 min, 3.12 μm/min within the period of the next 8 min (from min 4 to min 12), and 1.0 μm/min from min 12 to min 40, while that of glycerol was 11.3 μm/min within the first 4 min, 1.0 μm/min from min 4 to min 15 and 1.3 μm/min from min 16 to min 30, respectively. The plot shows that at the end of 4 min, DMSO rapidly penetrated into porcine skin at ~150 μm while glycerol was detected only at ~70 μm, even after 30 min. It is clear that DMSO has faster penetration into porcine skin than glycerol does. One possible reason is that the size of glycerol (with the molecular weight of 92.10) is larger than that of DMSO (with the molecular weight of 78.13), which has an effect on the penetration because of the brick-mortar structure of the stratum corneum that prevents large molecules from passing through. Additionally, compared with glycerol, the interaction between DMSO and the polar membrane surface affected the close packing of hydrocarbon chains of lipid molecules. The interaction between DMSO and the polar membrane surface gives rise to defects in the bilayer structure of skin tissue, which results in the increase of DMSO permeability.

To summarize, current results from the FTIR spectroscopic imaging technique showed the dynamic penetration process of DMSO and glycerol within porcine skin tissue. At the same time, the results also revealed that DMSO possesses the faster penetration rate than that of glycerol, which agreed well with previous studies.[19] Fast penetration is particularly important for *in-vivo* applications, because it could create a rapid refrac-

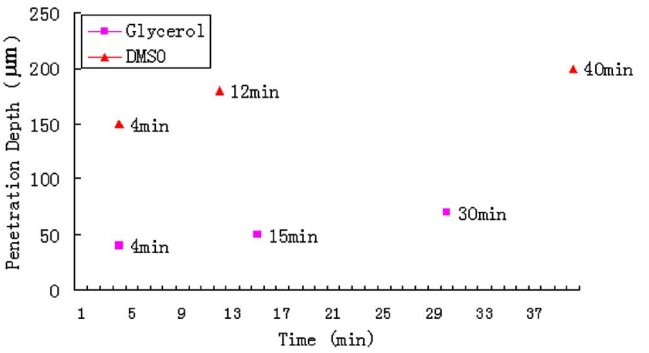

Fig. 9 Penetration depths of DMSO and glycerol into porcine skin over time. (Color online only.)

tive index matching environment within tissue that would consequently lead to an improvement in light penetration depth, benefiting a number of optical techniques, for example *in-vivo* optical imaging of biological tissues.[23]

5 Conclusion

We show that the FTIR spectroscopic imaging technique is a powerful analytical tool for investigation penetration kinetics of agents within tissue. Furthermore, both IR spectroscopic images and 3-D false color plots can be used to show the penetration kinetics through grayscale mode or false color mode. With appropriate image processing techniques, quantification of kinetic penetration of optical clearing agents into the different tissues is therefore possible. The current results demonstrate that FTIR spectroscopic imaging is not only useful for our further understanding of tissue optical clearing dynamics of glycerol and DMSO, but also could further provide an opportunity to quantify hyperosmotically biocompatible agents used for the optical clearing of different biological tissues. Therefore, FTIR spectroscopic imaging techniques may have great potential in further studies of optical clearing approaches in applications for light-based therapeutic and diagnostic techniques, as well as optical imaging techniques.

Acknowledgments

This research was supported in part by the Engineering and Physical Science Research Council, United Kingdom, under the project GR/R52978. J.J. acknowledges the K. C. Wong Fellowship of the Royal Society (United Kingdom) and the support from the National Natural Science Foundation of China (NSFC, number 30600126). The results presented in this work were collected when Jiang and Wang were at the Institute of Bioscience and Technology, Cranfield University, United Kingdom.

References

1. V. V. Tuchin, I. L. Maksimova, D. A. Zimnyakov, I. L. Kon, A. H. Mavlutov, and A. A. Mishin, "Light propagation in tissues with controlled optical properties," *J. Biomed. Opt.* **2**(4), 401–407 (1997).
2. J. Jiang and R. K. Wang, "Synergistic effect of hyperosmotic agents undertopical application on optical clearing of skin tissue in vitro, *Proc. SPIE* **5696**, 80–90 (2005).
3. X. Xu, R. K. Wang, J. B. Elder, and V. V. Tuchin, "Effect of dextran-induced changes in refractive index and aggregation on optical properties of whole blood," *Phys. Med. Biol.* **48**, 1205–1221 (2003).
4. H. Liu, B. Beauvoit, M. Kimura, and B. Chance, "Dependence of tissue optical properties on solute-induced changes in refractive index and osmolarity," *J. Biomed. Opt.* **1**(2), 200–211 (1996).
5. V. V. Tuchin, X. Xu, and R. K. Wang, "Dynamic optical coherence tomography in optical clearing, sedimentation and aggregation study of immersed blood," *Appl. Opt.* **41**, 258–271 (2002).
6. R. K. Wang, X. Xu, V. V. Tuchin, and J. B. Elder, "Concurrent enhancement of imaging depth and contrast for optical coherence tomography by hyperosmotic agents," *J. Opt. Soc. Am. B* **18**, 948–953 (2001).
7. R. K. Wang and J. B. Elder, "Propylene glycerol as a contrasting agent for optical coherence tomography to image gastro-intestinal tissues," *Lasers Surg. Med.* **30**, 201–208 (2002).
8. J. Jiang and R. K. Wang, "Comparing synergistic effects of oleic acid and dimethyl sulfoxide as vehicle on optical clearing of skin tissue in vitro," *Phys. Med. Biol.* **49**, 5283–5294 (2004).
9. G. Vargas, E. K. Chan, J. K. Barton, H. G. Rylander, and A. J. Welch, "Use of an agent to reduce scattering in skin," *Lasers Surg. Med.* **24**, 133–144 (1999).
10. S. Plotnikov, V. Juneja, A. B. Isaacson, W. A. Mohler, and P. J. Campagnola, "Optical clearing for improved contrast in second harmonic generation imaging of skeletal muscle," *Biophys. J.* **90**, 328–339 (2006).
11. R. Bhargava, B. G. Wall, and J. L. Koenig, "Comparison of the FTIR mapping and imaging techniques applied to polymeric systems," *Appl. Spectrosc.* **54**, 470–479 (2000).
12. E. N. Lewis, A. M. Gorbach, C. Marcott, and I. W. Levin, "High-fidelity Fourier transform infrared spectroscopic imaging of primate brain tissue," *Appl. Spectrosc.* **50**, 263–269 (1996).
13. M. van de Weert, R. van't Hof, J. van der Weerd, R. M. A. Heeren, G. Posthuma, W. E. Hennink, and D. J. A. Crommelin, "Lysozyme distribution and conformation in a biodegradable polymer matrix as determined by FTIR techniques," *J. Controlled Release* **68**, 31–40 (2000).
14. T. Ribar, J. L. Koenig, and R. Bhargave, "FTIR imaging of polymer dissolution. 2. Solvent/nonsolvent mixtures," *Macromolecules* **34**, 8340–8346 (2001).
15. J. Gonzalez-Benito and J. L. Koenig, "FTIR imaging of the dissolution of polymers. 4. Poly(methyl methacrylate) using a cosolvent mixture (carbon tetrachloride/methanol)," *Macromolecules* **35**, 7361–7367 (2002).
16. D. W. Eafferty and J. L. Koenig, "FTIR imaging for the characterization of controlled-release, drug delivery applications," *J. Controlled Release* **83**, 29–39 (2002).
17. K. H. Kolb, G. Janicke, M. Kramer, P. E. Schulze, and G. Raspe, "Absorption, distribution and elimination of labelled dimethyl sulfoxide in man and animals," *Ann. N.Y. Acad. Sci.* **141**, 85–95 (1967).
18. M. S. Frank, M. C. Nahata, and M. D. Hilty, "Glycerol: a review of its pharmacology, pharmacokinetics, adverse reactions, and clinical use," *Pharmacotherapy* **1,2**, 147–160 (1981).
19. Y. He and R. K. Wang, "Dynamic optical clearing effect of tissue impregnated with hyperosmotic agents and studied with optical coherence tomography," *J. Biomed. Opt.* **9**(1), 200–206 (2004).
20. M. B. Sulzberger, T. A. Cortese, and L. Fishman, "Some effects of DMSO on human skin in vivo," *Ann. N.Y. Acad. Sci.* **140**, 437–506 (1966).
21. S. V. Rudenko, S. D. Gapochenko, and V. A. Bondarenko, "Effect of glycerol on the capacitance and conductivity of bilayer lipid membranes," *Biophysics (Engl. Transl.)* **29**, 245–249 (1984).
22. R. B. Stoughton and W. Fritsch, "Influence of dimethyl sulfoxide on human percutaneous absorption," *Arch. Dermatol.* **90**, 512–517 (1964).
23. H. Zhao, F. Gao, Y. Tanikawa, K. Homma, and Y. Yamada, "Time-resolved diffuse optical tomographic imaging for the provision of both anatomical and functional information about biological tissue," *Appl. Opt.* **44**(10), 906–1916 (2005).